Kairn, Tanya and Kenny, John and Crowe, Scott and Fielding, Andrew L. and Franich, Rick and Johnston, Peter and Knight, Richard and Langton, Christian M. and Schlect, David and Trapp, Jamie (2010) ***Technical note : modelling a complex micro-multileaf collimator using the standard BEAMnrc distribution.*** Medical Physics, 37(4). pp. 1761-1767.

Technical note: Modelling a complex micro-multileaf collimator using the standard BEAMnrc distribution

T. Kairn[1],* J. Kenny[2], S. B. Crowe[1], A. L. Fielding[1], R. D. Franich[3], P. N. Johnston[4], R. T. Knight[2], C. M. Langton[1], D. Schlect[2], and J. V. Trapp[1]

[1] *School of Physical and Chemical Sciences, Queensland University of Technology, GPO Box 2434, Brisbane Qld 4001, Australia*

[2] *Premion, The Wesley Medical Centre, Suite 1, 40 Chasely St, Auchenflower, Qld 4066, Australia*

[3] *School of Applied Sciences, RMIT University, GPO Box 2476, Melbourne, Vic 3001, Australia and*

[4] *Australian Radiation Protection and Nuclear Safety Agency, 619 Lower Plenty Road, Yallambie, Vic 3085, Australia*

(Dated: January 15, 2010)

Abstract

The component modules in the standard BEAMnrc distribution may appear to be insufficient to model micro-multileaf collimators that have tri-faceted leaf ends and complex leaf profiles. This note indicates, however, that accurate Monte Carlo simulations of radiotherapy beams defined by a complex collimation device can be completed using BEAMnrc's standard VARMLC component module. That this simple collimator model can produce spatially and dosimetrically accurate micro-collimated fields is illustrated using comparisons with ion chamber and film measurements of the dose deposited by square and irregular fields incident on planar, homogeneous water phantoms. Dose calculations for on- and off-axis fields are shown to produce good agreement with experimental values, even upon close examination of the penumbrae. Simulation parameters are provided which should allow other researchers to adapt and use this model to study clinical stereotactic radiotherapy treatments.

*Electronic address: t.kairn@qut.edu.au

I. INTRODUCTION

Micro-multileaf collimators (μMLCs) are used in stereotactic photon-beam radiotherapy and radiosurgery. Although they are increasingly used in treatments of extra-cranial targets, the predominant use of μMLCs is in the treatment of cancers and non-malignant lesions in the brain. Because cranial treatment sites are usually very small, highly collimated fields are required, to maximally spare all adjacent healthy tissue [1]. The BrainLAB m3 μMLC (BrainLAB, Feldkirchen, Germany) fulfills this requirement by deploying leaves that project to widths that can be as small as 0.3 cm, at the linear accelerator isocentre [2, 3], with narrow penumbrae. The accurate prediction of dose delivered by such small fields is a challenge suited to examination through Monte Carlo simulation [4–7], which can be carried out using the BEAMnrc code [8, 9].

Given the importance of peripheral and penumbral features for these small fields, the effects of leaf-end and leaf-edge geometries must be reproduced accurately in the Monte Carlo model. The leaf edge shape of the BrainLAB m3 μMLC consists of three tongues and three grooves along each leaf side, with all leaf edges focussed towards the photon source. Each leaf end consists of three planar facets that are angled to match the divergence of the beam at the extremes of the leaf's motion ($\pm 2.86^o$ from vertical) as well as on the central axis (0^o from vertical). The 26 pairs of leaves in the m3 μMLC's leaf-banks vary in thickness from 0.3 cm for the central 14 pairs of leaves, to 0.45 cm for the adjacent 6 pairs of leaves, to 0.55 cm for the outer 6 pairs of leaves (when all distances are projected to the isocentre).

Several stereotactic radiotherapy collimation systems can be modelled precisely using component modules in the standard BEAMnrc distribution. For example, the Elekta Synergy (Elekta Ltd, Crawley, UK) and MRC ModuLeaf (MRC Systems GmbH, Heidelberg, Germany) miniature MLCs can both be modelled using BEAMnrc's MLCE component module [10–12]. Cylindrical micro-collimation systems can be modelled using various other BEAMnrc component modules (including CONESTAK, CONS3R and FLATFILT) [13, 14]. However, the geometry of the BrainLAB m3 μMLC cannot be modelled exactly, in full detail, using standard BEAMnrc component modules [5]. For instance, both VARMLC and DYNVMLC allow the modelling of: complex details of leaf edges; leaf focussing towards the photon source; leaves of different widths within the one MLC; and leaves with either flat or curved leaf ends [15]. However, neither module permits the modelling of leaves with flat

ends without varying the end shape with field size, or leaves with three tongues and three grooves along each side [5, 6].

To approximate the complex geometry of the BrainLAB m3 μMLC, Belec *et al* [5] have produced a modified component module for use with BEAMnrc which is based on VARMLC and allows the modelling of flat, unvarying leaf ends. The layering of three of these component modules allows the facets of the m3 μMLC's leaf ends to be modeled accurately, for all leaf positions. Additionally, Belec *et al* [5] have shown that careful selection of input parameters allows these component modules to be used to model leaves that each have three tongues and one groove on one side and three grooves and one tongue on the other. This irregular shape has been shown to accurately reproduce the interleaf leakage from the Brainlab m3 device [5]. Belec et al [5]'s modified VARMLC module is, however, not available through the standard BEAMnrc distribution.

The component modules in the standard BEAMnrc distribution (such as VARMLC) do not permit such precise modelling of the details of the μMLC's geometry. However, this note aims to establish that the standard VARMLC component module can be used to produce a beam which conforms to the output of the clinical μMLC device.

The use of a standard BEAMnrc component module is advantageous because the BEAMnrc codes are freely and widely distributed, have been thoroughly established as being reliable and accurate, are fully documented and supported by the National Research Council Canada, and are specifically designed to compile and run successfully on a wide range of platforms and systems. This accessibility is a major advantage of using the standard BEAMnrc codes.

II. MODEL

When using VARMLC to model the m3 μMLC, two major simplifications are involved. Firstly, the tri-faceted shape of the μMLC leaf ends is simplified into a curve and, secondly, the three tongues and three grooves along each μMLC leaf edge are modelled as a single tongue and groove in each leaf.

Figure 1 illustrates the geometric effect of combining the three angled surfaces at the end of each μMLC leaf into a single curve. The radius of this curve is determined using the

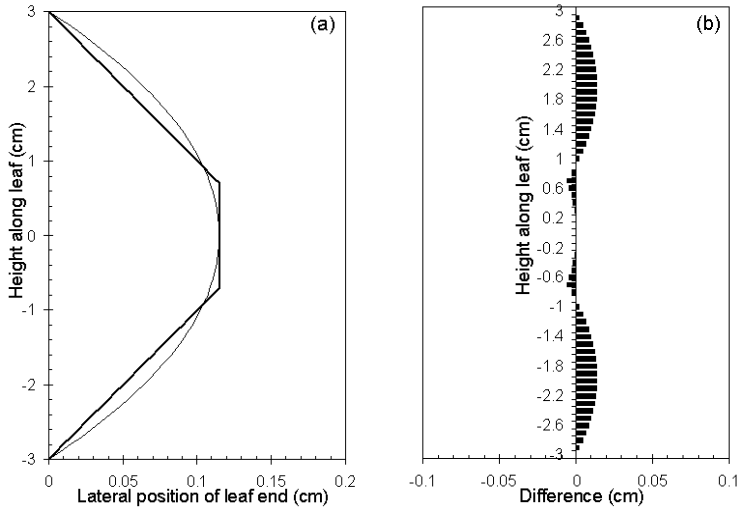

FIG. 1: Comparison of μMLC leaf end shape illustrated as (a) shape of curved leaf end (light, solid line) superimposed on shape of angled leaf end (heavy, solid line) and (b) difference (in centimetres) between lateral positions of rounded and angled leaves, at each height along the leaf. (To make these differences visible, the horizontal scale on each figure is exaggerated, compared to the vertical.)

following geometric relationship:

$$RADIUS = \frac{T_{leaf}^2 + 4(T_{section}tan(\theta))^2}{8T_{section}tan(\theta)}, \tag{1}$$

where T_{leaf} is the total (vertical) thickness of the μMLC leaf, $T_{section}$ is the thickness of the angled section of the leaf (see Figure 1), and θ is the angulation of the angled section (the beam divergence at maximum field size, $\theta = 2.86^o$). As Figure 1 shows, the maximum spatial difference between a point on a tri-faceted leaf end and a point at the same height (distance from the photon source) on the suggested curved leaf is 0.014 cm. However, the effects of the small physical differences illustrated in Figure 1(b) are mitigated by the use of leaf position offset corrections in the setting of both the simulated μMLC leaf positions and the positions of the leaves in clinical treatments. In the BEAMnrc model, the position (P) of a given μMLC leaf tip is defined by

$$P = L - \left(RADIUS - \frac{RADIUS}{H}\sqrt{L^2 + H^2} \right) \tag{2}$$

where $RADIUS$ is the radius of curvature of the leaf (see Table I), L is the length of the light field (measured from the central axis) defined by that leaf, H is the height (distance from

the source) of the μMLC leaf-bank and all values are measured at the μMLC midplane. The bracketed terms in Equation 2 define an offset that allows for the collimation of the beam by regions (a) below the centre of the leaf, when the leaf is opened away from the central axis, and (b) above the centre of the leaf, when the leaf is closed across the central axis. (When applying Equation 2, positive values of L should be used in case (a), and negative values of L in case (b).) The shape of the leaf ends in the clinical μMLC is similarly accounted for, using a field size dependent offset, so that in both the simulation model and the experimental system, the size of the light field produced by the μMLC matches the size of the planned radiation field.

A complex leaf edge design is incorporated into the design of of the BrainLAB m3 μMLC for mechanical, rather than dosimetric, reasons [2]. Whereas a single tongue and groove in each leaf might be sufficient to minimise interleaf leakage (as in the Siemens 29-leaf and the Varian 52-leaf MLCs [16]), it was necessary to incorporate three tongues and grooves into the design of each side of the m3 μMLC in order to offset each leaf's drive shaft and optimise the position of the driving motors, in this very confined geometry [2].

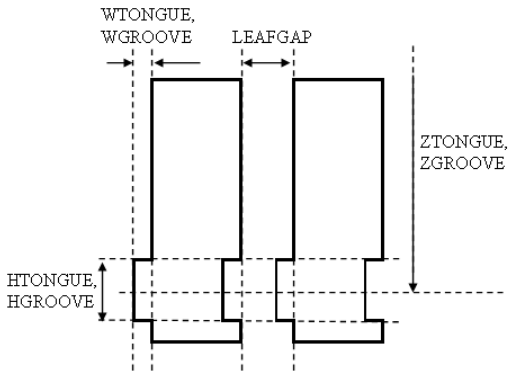

FIG. 2: Basic geometry of VARMLC leaf edges, as used in the m3 μMLC model. (Not to scale.) $ZTONGUE$ and $ZGROOVE$ are measured from the top of the component module.

Due to the limitation that the VARMLC component module allows for only one tongue and groove per leaf [9], our model of the m3 μMLC was designed with that simplification (see Figure 2). The position ($ZTONGUE$ and $ZGROOVE$), width ($WTONGUE$ and $WGROOVE$) and height ($HTONGUE$ and $HGROOVE$) of this tongue and groove were optimised by comparing virtual film images obtained via simulation of a field produced with open linear accelerator jaws and closed μMLC leaves, with a commensurate clinical image

(obtained as described below), where all data were normalised to the central axis dose for a 10×10 cm^2 field. The relevant simulation parameters were varied until the resulting virtual image exhibited peaks (interleaf leakage) and troughs (leaf transmission) which matched the experimental film in both their period and peak location. As shown in Figure 3, the matching of the amplitudes of these dose oscillations was only approximate. The maximum difference between dose peaks measured using film and modelled using Monte Carlo is almost 20 % (labelled 'A' in Figure 3(a)) and the maximum difference between troughs measured with film and modelled using Monte Carlo is greater than 6 % (labelled 'B' in Figure 3(a)). These discrepancies were accepted because, as Figure 3(a) suggests, variations in measured dose (arising from either variations in the film's response to this low dose field [17] or variations in the sizes of the gaps between each leaf and its neighbour) can be estimated at up to ± 12 % of the dose delivered, so a close match between measurement and simulation would be untenable. (This approximate matching produces a model capable of reliably simulating the edges of single fields, as exemplified by data shown in Figure 3(b), but also capable of under-representing the 'tongue and groove effect' [18], as shown in Figure 3(c), which should be considered when combining multiple fields.) The accuracy of the model obtained by this means can be confirmed through examination of the verification results discussed in the next section.

Table I lists the optimised values of the parameters that were varied during this commissioning process, as well as the various constants that define the VARMLC m3 μMLC model. The data in Table I should not be read as an accurate description of the internal geometry of the BrainLAB m3 μMLC. Rather, these are an example of a set of simulation parameters that can be used to produce a model of the m3 μMLC which replicates the output of the clinical device. These values may also be taken as a set of initial parameters and used in the commissioning of VARMLC models of local m3 μMLC devices at other centres.

In this work, the Varian Clinac 21iX linear accelerator (Varian Medical Systems, Palo Alto, USA), operating at 6 MV, was modelled in a separate BEAMnrc simulation, producing a phase-space file 55 cm from the photon source. The resulting data were used as input for a series of BEAMnrc simulations of the BrainLAB m3 μMLC. The Virtual Water (Standard Imaging, Middleton, USA) and Gafchromic EBT2 dosimetry film (International Specialty Products, Wayne, USA) used to obtain experimental images were modelled using the composition of Virtual Water reported by McEwen and Niven [19] embedded with a 0.2 mm

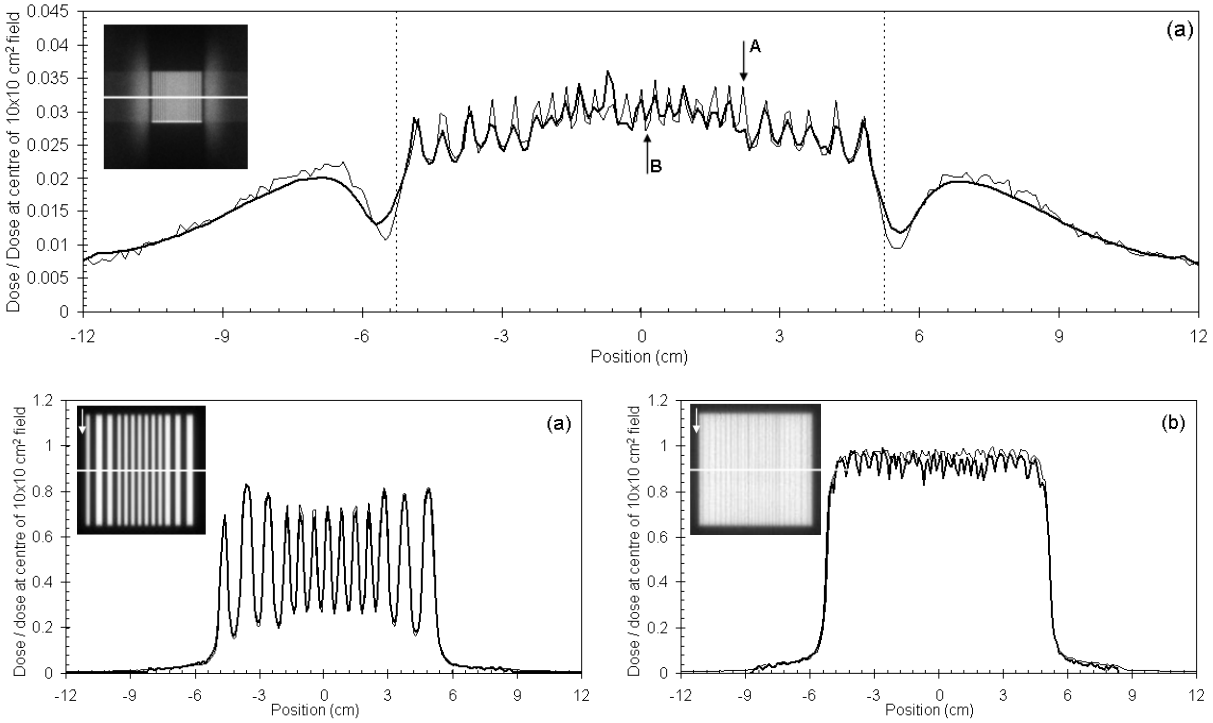

FIG. 3: Comparison of dose profiles from film (heavy lines) and simulation (light lines), showing: (a) profiles across the closed-leaf field (labels 'A' and 'B' indicate points of strongest disagreement); (b) profiles across the alternating closed and open leaf field; and (c) profiles across the sum of a field with even numbered leaves closed and a field with odd numbered leaves closed (tongue and groove effect). Doses are normalised to the central axis dose for a 10×10 cm^2 field. Vertical dotted lines in (a) indicate jaw positions. The insets show (a) a 30×30 cm^2 image of the field, and (b) and (c) 12×12 cm^2 images of the fields, where white lines indicate the locations of the profiles.

thick layer of polyester. The lateral area of the voxels used in the simulations was 0.1×0.1 cm^2.

The film was scanned on an Epson Perfection V700 Photo flatbed scanner (Seiko Epson Corp., Nagano, Japan), using a novel setup designed to minimise interference and improve dose-calculation reliability [20]. Briefly, each scan of the of EBT2 film was made with the film placed on a plastic frame containing a 17×17 cm^2 aperture, so that the film could be kept out of contact with the glass surface of the scanner. These scans were made before and after irradiation and were used, along with calibration measurements and scans of the plastic frame, to determine maps of net optical density, which were corrected for variations

TABLE I: Modelling the m3 μMLC using VARMLC: Values of parameters that were held constant and final values of parameters that were varied during model optimisation. Here, $number_i$ denotes the number of leaf pairs of type i, $width_i$ denotes the width of each leaf of type i measured at the top of the μMLC leaf-bank and all other parameter names are as defined by Rogers *et al* [9]

Constant parameters		Variable parameters	
$ZMIN$	4.0	$WSCREW$, $HSCREW$	0.0
$ZTHICK$	6.0	$ZTONGUE$, $ZGROOVE$	8.7
$ZFOCUS$	-55.0	$HTONGUE$, $HGROOVE$	2.20
$RADIUS$	39.19	$WTONGUE$, $WGROOVE$	0.003
$NGROUP$	5	$LEAFGAP$	0.003
$number_1$	3	$width_1$	0.3230
$number_2$	3	$width_2$	0.2640
$number_3$	14	$width_3$	0.1755
$number_4$	3	$width_4$	0.2640
$number_5$	3	$width_5$	0.3230

in scanner output and film response, and which were converted to dose. In these analyses only red-channel data were used; our procedure does not include the blue-channel correction recommended by the manufacturer. Initial experience with EBT2 film indicates that there is a noticeable variation in blue channel response between film batches and suggests that the blue-channel correction adds little value and may introduce additional noise [20].

Further dose measurements were obtained experimentally by adaptively step-scanning (with a minimum step size of 0.05 cm) using an A16 Exradin MicroChamber (Standard Imaging, Middleton, USA) in a Scanditronix-Wellhofer Blue Water Phantom (IBA dosimetry, Louvain-la-Neuve Belgium). The A16 microchamber has a collecting volume of 0.007 cm^3, enclosed in a shell with an external diameter of 0.34 cm, and has been shown to produce accurate measurements of dose from fields down to 1×1 cm^2 [21]. This system was modelled for Monte Carlo calculations as a $60 \times 60 \times 60$ cm^3 volume of water.

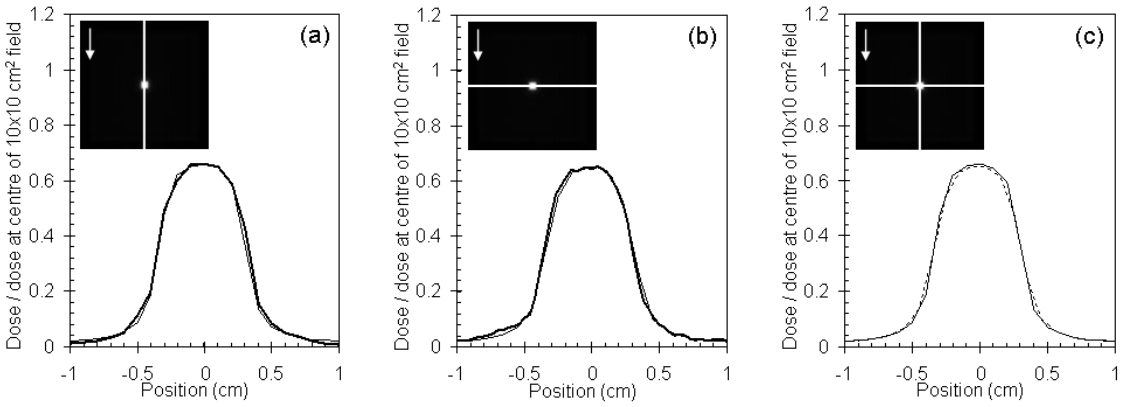

FIG. 4: Comparison of dose profiles across a 0.6×0.6 cm^2 square, on-axis field, from film (heavy lines) and simulation (light lines), showing: (a) profiles in the direction of μMLC motion; (b) profiles in the direction orthogonal to μMLC motion; and (c) a comparison of simulation profiles in the directions orthogonal (dotted line) and parallel (solid line) to μMLC motion. Doses are normalised to the central axis dose for a 10×10 cm^2 field. Jaws were set at 9.8×9.8 cm^2. Insets show a 12×12 cm^2 image of the fields, from the Monte Carlo simulation, where white lines indicate the locations of the profiles and arrows show the direction of leaf motion.

III. VERIFICATION

To initially verify the dosimetric accuracy of the fields produced by the VARMLC Monte Carlo model of the BrainLAB m3 μMLC comparisons were made between relative dose profiles in water from experiment (using both ion chamber and film measurements) and simulation, for square fields varying in size from 10×10 cm^2 down to 0.6×0.6 cm^2. Beyond a depth of 0.3 cm, all depth-dose profiles from simulation were found to be in agreement, within 1.2%, with profiles obtained experimentally. For the smallest field, agreement along the depth-dose curve was within 1%. All lateral profiles showed similar agreement, differing by less than 1%, except at the outer edges of the penumbrae (beyond the 20% isodose) of fields smaller than 1×1 cm^2. These very small fields, however, did show agreement within 1% across this region when compared with experimental film data. Figures 4(a), (b) and (c) exemplify the agreement between the film data and simulation results, for very small fields, and illustrate a consistency of penumbra width in directions parallel and orthogonal to μMLC motion that has been previously identified in film-based analyses of BrainLAB

m3 μMLC fields [22]. (Further examples of comparisons between simulation and experimental (film and ion chamber) results can be found in supplemental material accessible from http://scitation.aip.org/medphys/.)

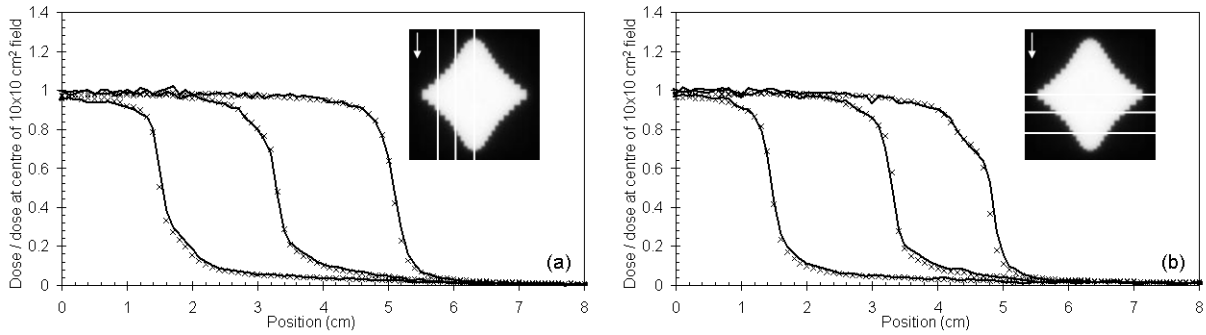

FIG. 5: Comparison of dose profiles across a diamond-shaped quality assurance field, from film (heavy lines) and simulation (crosses), showing: (a) overlaid profiles in the direction of μMLC motion; and (b) overlaid profiles in the direction orthogonal to μMLC motion. Doses are normalised to the central axis dose for a 10×10 cm^2 field. Jaws were set at 9.8×9.8 cm^2. Insets show a 12×12 cm^2 image of the fields, from the Monte Carlo simulation, where white lines indicate the locations of the profiles and arrows show the direction of leaf motion.

To further test the possible effects of the VARMLC model's simplified leaf ends and leaf edges on the shape of field penumbrae, profiles through a range of leaf openings in a diamond-shaped quality assurance field were examined (see Figure 5). The penumbra widths were measured (between 20 and 80 % of the maximum in each profile) and for each of the 24 different widths of this field in each direction. All of the penumbra widths obtained from the simulation were within 1 mm of the corresponding penumbra widths obtained from the film image. Figure 5 illustrates some examples of these penumbrae, comparing film measurements and simulation results. There are localised deviations between the measured and simulated data shown in these profiles, but these do not appear to be systematic. Generally, 99.7 % of pixels in the virtual image agree with the experimental image, within strict gamma acceptance criteria (2%, 1mm) [23].

These results suggest that the simplifications involved in the development of the VARMLC model of the BrainLAB m3 μMLC do not necessarily affect the accurate simulation of field edges. To further test this observation, the analysis was extended to the

examination of a series of very small, off-axis fields.

Insets in Figure 6 show a single field containing four small off-axis apertures, which was imaged using film and simulation. The chosen apertures include the smallest square fields available, given the geometry of the μMLC: The sizes were 0.6×0.6 cm^2 (two 0.3 cm leaves open), 0.55×0.55 cm^2 (one 0.55 cm leaf open), 0.45×0.45 cm^2 (one 0.45 cm leaf open), and 0.55×0.55 cm^2 (one 0.55 cm leaf open), and the (x, y) offsets were (-0.3,0.3), (4.18,-4.28), (-2.68,2.78) and (1.55,-1.65), respectively. Profiles across all of these apertures, in directions parallel and perpendicular to leaf motion, are shown in Figure 6.

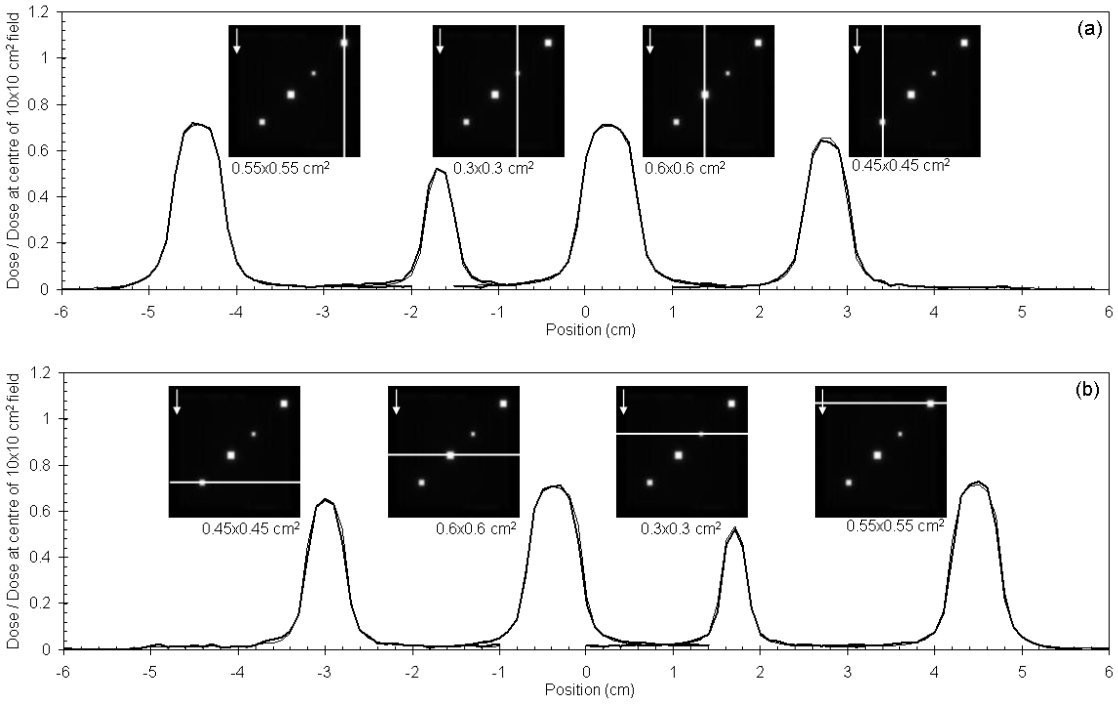

FIG. 6: Comparison of dose profiles across small offset fields, from film (heavy line) and simulation (light line), showing: (a) overlaid profiles in the direction of μMLC motion; and (b) overlaid profiles in the direction orthogonal to μMLC motion. Doses are normalised to the central axis dose for a 10×10 cm^2 field. Jaws were set at 9.8×9.8 cm^2. Insets show a 12×12 cm^2 image of the fields, from the Monte Carlo simulation, where white lines indicate the locations of the profiles and arrows show the direction of leaf motion.

The profiles in the leaf-motion direction shown in Figure 6(a) exemplify the results obtainable, when one leaf is translated across the central axis, and the resulting field is effectively being collimated by the upper region of the curved leaf end (shown in the region between 0

and 3 cm on the vertical axis of Figure 1). The agreement between the data obtained from measurement and simulation indicates that the VARMLC model is reliably able to replicate the collimating effect of the BrainLAB m3 μMLC, from situations when one leaf abutting the central axis (the 0.6×0.6 cm^2 field) to when both leaves are close to the limit of their motion (the 0.55×0.55 cm^2 field). The profiles in the direction orthogonal to leaf motion, shown in Figure 6(b) provide further confirmation of the suitability of the simplified tongue and groove in the VARMLC model. Across the whole field, 99.9 % of pixels in the simulated image agree with the experimental image, within 2%, 1mm acceptance criteria. Again, there is no systematic deviation at the penumbrae.

The agreement between simulation and experiment in these examples can be regarded as confirmation that the simplified leaf edges and leaf ends used in our VARMLC model are suitably replicating the effects of the more complex design of the clinical μMLC device.

IV. CONCLUSION

The Brainlab m3 μMLC device can be modelled using the standard BEAMnrc component module, VARMLC. Although the model itself relies on two major simplifications, the output it produces is spatially and dosimetrically accurate and agrees well with experimental measurements.

It is therefore possible to recommend the use of a VARMLC model of the m3 μMLC , along with a commissioned model of the associated Varian linear accelerator, to simulate stereotactic radiotherapy and radiosurgery treatments. The use of this simplified model takes advantage of the accessibility of the BEAMnrc code and its standard component modules and stands as a useful alternative to the development or application of an in-house or third-party component module.

Acknowledgments

This work was funded by the Wesley Research Institute, Australia (grant number 2008/11). Computational resources and services used in this work were provided by the High Performance Computing and Research Support Unit, Queensland University of Technology (QUT), Brisbane, Australia. The model Varian Clinac 21iX linac used in this study was

designed and commissioned by the authors with the assistance of M. Kakakhel of QUT, with reference to manufacturing specifications generously provided by Varian Medical Systems, Palo Alto, USA. The authors wish to thank M. L. Taylor of RMIT University, Melbourne, Australia, for the provision of physical measurements of the μMLC geometry, and T. Aland of Premion, Brisbane, Australia, for assistance in calibrating and analysing radiochromic film images. The authors are also grateful to J. Belec of Ottawa Hospital, Ottawa, Canada, H. Patrocinio of McGill University, Montreal, Canada, and F. Verhaegen of MAASTRO Clinic, Maastricht, Netherlands, for useful discussions regarding the geometry of the BrainLAB μMLC.

---

[1] M. C. Schell, F. J. Bova, D. A. Larson, D. D. Leavitt, W. R. Lutz, E. B. Podgorsak, A. Wu, *AAPM Report No 54: Stereotactic Radiosurgery* (Americal Institute of Physics Inc, Woodbury, 1995)

[2] V. P. Cosgrove, U. Jahn, M. Pfaender, S. Bauer, V. Budach, R. E. Wurm, "Commissioning of a micro multileaf collimator and planning system for stereotactic radiosurgery", Radiotherapy and Oncology. **50**, 325-336 (1999)

[3] P. Xia, P. Geis, L. Xing, C. Ma, D. Findley, K. Forster, A. Boyer, "Physical characteristics of a miniature multileaf collimator", Med. Phys. **26**(1), 65-70 (1999)

[4] I. J. Das, C-W. Cheng, R. J. Watts, A. Ahnesjo, J. Gibbons, X. A. Li, J. Lowenstein, R. K. Mitra, W. E. Simon, T. C. Zhu, "Accelerator beam data commissioning equipment and procedures: Report of the TG-106 of the Therapy Physics Committee of the AAPM", Med. Phys. **35**(9), 4186-4215 (2008)

[5] J. Belec, H. Patrocinio, F. Verhaegen, "Development of a Monte Carlo model for the Brainlab microMLC", Phys. Med. Biol. **50**, 787-799 (2005)

[6] G. X. Ding, D. M. Duggan, C. W. Coffey, "Commissioning stereotactic radiosurgery beams using both experimental and theoretical methods", Phys. Med. Biol. **51**, 2549-2566 (2006)

[7] A. J. D. Scott, A. E. and Nahum, J. D. Fenwick, "Using a Monte carlo model to predict dosimetric properties of small radiotherapy photon fields", Med. Phys. **35**(10), 4671-4684 (2006)

[8] D. W. O. Rogers, B. A. Faddegon, G. X. Ding, C. -M. Ma, J. We, T. R. Mackie, "BEAM:

A Monte Carlo code to simulate radiotherapy treatment units", Med. Phys. **22**(5), 503-524 (1995)

[9] D. W. O. Rogers, B. Walters, I. Kawrakow, *BEAMnrc Users Manual* (Ionising Radiation Standards, National Research Council of Canada, Ottawa, 2004)

[10] M. Heydarian, K. Asnaashari, M. Allahverdi, D. A. Jaffray, "Dosimetric evaluation of a dedicated sterotactic linear accelerator using measurement and Monte Carlo simulation", Med. Phys. **35**(9), 3943-3954 (2008)

[11] F. Crop, N. Reynaert, G. Pittomvils, L. Paelinck, W de Gersem, C. de Wagter, L. Vakaet, W. de Neve, H. Thierens, "Monte Carlo modeling of the ModuLeaf miniature MLC for small field dosimetry and quality assurance of the clinical treatment planning system", Phys. Med. Biol. **52**, 3275-3290 (2007)

[12] J. van de Walle, C. Martens, N. Reynaert, H. Palmans, M. Coghe, W. de Neve, C de Wagter, H. Thierens, "Monte Carlo model of the Elekta SLiplus accelerator: validation of a new MLC component module in BEAM for a 6MV beam", Phys. Med. Biol. **48**, 371-385 (2003)

[13] J. Deng, T. Guerrero, C-M. Ma, R Nath, "Modelling 6 MV photon beams of a stereotactic radiosurgery system for Monte Carlo treatment planning", Phys. Med. Biol. **49**, 1689-1704 (2004)

[14] P. Francescon, S. Cora, C. Cavedon, "Total scatter factors of small beams: A multidetector and Monte Carlo study", Med. Phys. **35**(2), 504-513 (2008)

[15] E. Heath, J. Seuntjens, "Development and validation of a BEAMnrc component module for accurate Monte Carlo modelling of the Varian dynamic Millenium multileaf collimator", Phys. Med. Biol. **48**, 4045-4063 (2003)

[16] M. S. Huq, I. J. Das, T. Steinberg, J. M. Galvin, "A dosimetric comparison of verious multileaf collimators", Phys. Med. Biol. **47**, N159-N170 (2002)

[17] P. Francescon, S. Cora, C. Cavedon, P. Scalchi, S. Reccanello, F. Colombo, "Use of a new type of radiochromic film, a new parallel -plate micro-chamber, MOSFETs, and TLD 800 microcubes in the dosimetry of small beams" Med. Phys. **25**(4), 503-511 (1998)

[18] J. V. Siebers, P. J. Keall, J. O. Kim, R. Mohan, "A method for photon beam Monte Carlo multileaf collimator particle transport" Phys. Med. Biol. **47**: 3225-3249 (2002)

[19] M. R. McEwen, D. Niven, "Characterization of the phantom material Virtual WaterTM in high-energy photon and electron beams" Med. Phys. **33**(4), 876-887 (2006)

[20] J. Kenny, T. Aland, T. Kairn, "Evaluation of EBT2 gafchromic film dosimetry system as part of a RapidArc and IMRT commissioning and quality assurance program", in preparation, 2010.

[21] M. Stasi, B. Baiotto, G. Barboni, G. Scielzo, "The behaviour of several microionisation chambers in small intensity modulated radiotherapy fields." Med. Phys. **31**(10): 2792-2795 (2004)

[22] O. A. Garcia-Garduno, M. A. Celis, J. M. Larraga-Gutierrez, S. Moreno-Jimenez, A. Martinez-Davalos, M. Rodruiguez-Villafuerte, "Radiation transmission, leakage and beam penumbra measurements of a micro-multileaf collimator using GafChromic EBT film", J. Appl. Clin. Med. Phys. **9**(3): 90-98 (2008)

[23] M. Wendling, L. J. Zijp, L. N. McDermott, E. J. Smit, J.-J. Sonke, B. J. Mijnheer, M. van Herk, "A fast algorithm for gamma evaluation in 3D", Med. Phys. **34**(5), 1647-1654 (2007)